Recent History of Large-Scale Ecosystem Disturbances in North America Derived from the AVHRR Satellite Record

Christopher Potter,[1]* Pang-Ning Tan,[2] Vipin Kumar,[2] Chris Kucharik,[3] Steven Klooster,[4] Vanessa Genovese,[4] Warren Cohen,[5] and Sean Healey[5]

[1]*NASA Ames Research Center, Moffett Field, California 94035, USA;* [2]*University of Minnesota, Minneapolis, Minnesota 55415, USA;* [3]*University of Wisconsin, Madison, Wisconsin 53706, USA;* [4]*California State University Monterey Bay, Seaside 93955, California, USA;* [5]*USDA Forest Service, Corvallis, Oregon 97331, USA*

ABSTRACT

Ecosystem structure and function are strongly affected by disturbance events, many of which in North America are associated with seasonal temperature extremes, wildfires, and tropical storms. This study was conducted to evaluate patterns in a 19-year record of global satellite observations of vegetation phenology from the advanced very high resolution radiometer (AVHRR) as a means to characterize major ecosystem disturbance events and regimes. The fraction absorbed of photosynthetically active radiation (FPAR) by vegetation canopies worldwide has been computed at a monthly time interval from 1982 to 2000 and gridded at a spatial resolution of 8–km globally. Potential disturbance events were identified in the FPAR time series by locating anomalously low values (FPAR-LO) that lasted longer than 12 consecutive months at any 8-km pixel. We can find verifiable evidence of numerous disturbance types across North America, including major regional patterns of cold and heat waves, forest fires, tropical storms, and large-scale forest logging. Summed over 19 years, areas potentially influenced by major ecosystem disturbances (one FPAR-LO event over the period 1982–2000) total to more than 766,000 km^2. The periods of highest detection frequency were 1987–1989, 1995–1997, and 1999. Sub-continental regions of the Pacific Northwest, Alaska, and Central Canada had the highest proportion (>90%) of FPAR-LO pixels detected in forests, tundra shrublands, and wetland areas. The Great Lakes region showed the highest proportion (39%) of FPAR-LO pixels detected in cropland areas, whereas the western United States showed the highest proportion (16%) of FPAR-LO pixels detected in grassland areas. Based on this analysis, an historical picture is emerging of periodic droughts and heat waves, possibly coupled with herbivorous insect outbreaks, as among the most important causes of ecosystem disturbance in North America.

Key words: ecosystem disturbance; remote sensing; fire; drought; forests.

INTRODUCTION

Ecosystem structure and function are strongly impacted by major disturbance events (Pickett and White 1985; Walker and Willig 1999), many of which in North America are associated with sea-

sonal temperature extremes, droughts, wildfires, and tropical storms. Potter and others (2003a,b) characterized a large scale ecological disturbance as an event that results in a sustained disruption of ecosystem structure and function generally with effects that last for time periods longer than a single seasonal growth cycle for native vegetation. Physical disturbance categories include fires, hurricanes, floods, droughts, lava flows, and ice storms. Biogenic disturbance categories include the impacts of herbivorous insects, mammals, and pathogens. Anthropogenic disturbance categories include logging, deforestation, drainage of wetlands, clearing for cultivation, chemical pollution, and alien species introductions. Many of these events alter ecosystem productivity and resource availability (light and nutrients) for organisms on large spatial and temporal scales (Pickett and White 1985; Tilman 1985).

Ecosystem disturbances can contribute to the current rise of carbon dioxide (CO_2) levels in the atmosphere (Schimel and others 2001). Because major 'pulses' of CO_2 and other trace gases from terrestrial biomass loss can be emitted to the atmosphere during large disturbance events, the timing, location, and magnitude of vegetation disturbance is presently a major uncertainty in understanding global biogeochemical cycles (Canadell and others 2000). Numerous studies have been conducted to quantify carbon emissions from single categories of disturbance, principally biomass burning events, and generally with national or continental levels of resolution. These studies include Kurz and Apps (1999), Houghton and others (1999), Murph and others (2000), Amiro and others (2001) for portions of North America, Fearnside (1997), Nepstad and others (1999), Potter and others (2001) for portions of South America, Scholes and others (1996), Barbosa and others (1999) for portions of Africa, Houghton and Hackler (1999) for portions of Southeast Asia, and Hurst and others (1994) for Australia. Several studies have dealt with global level effects of deforestation of carbon emissions (Andreae 1991; Houghton 1999; Potter 1999).

Potter and others (2003a) reported an approach for detection of large-scale ecosystem disturbance (LSEDs) events based on sustained declines in vegetation greenness observed by daily satellite observations. This approach was global in scope, covered more than a decade of analysis, and encompassed all potential categories of major ecosystem disturbance—physical, biogenic, and anthropogenic—using a consistent method of detection and analysis. This method was based on

the 18-year record of global satellite observations of vegetation phenology from the advanced very high resolution radiometer (AVHRR) as a time series to characterize major ecosystem disturbance events and regimes. The fraction absorbed of photosynthetically active radiation (FPAR) by vegetation canopies worldwide was computed at a monthly time interval from 1982 to 1999 and gridded at a spatial resolution of 0.5° latitude/longitude. Potential disturbance events of large extent (greater than a single 8-km pixel area of 6400 ha) were identified in the FPAR time series by locating anomalously low values (FPAR-LO) that lasted longer than 12 consecutive months at any pixel. Potter and others (2003a) reported that nearly 400 Mha of the global land surface could be identified with at least one FPAR-LO event over the 18-year time series. The majority of these potential disturbance events occurred in tropical savanna and shrublands or in boreal forest ecosystem classes. Verification of potential disturbance events from the FPAR-LO analysis was carried out using documented records of the timing of large-scale wildfires at locations throughout the world. Disturbance regimes were further characterized by association analysis with historical climate events worldwide.

This FPAR-LO detection approach is based on the concept that leafy vegetation cover is likely the most fragile and therefore perhaps the single most vulnerable biotic component of terrestrial ecosystems to detectable alteration during major disturbance events. Vegetation leaf cover burns relatively easily or can be readily blown down, cut to the ground, or defoliated by herbivores. Leaf litter then decomposes rapidly to blend in with background soil attributes, at least compared to the large woody biomass components of shrub, woodland, and forest ecosystems.

Earth-observing satellites have monitored daily leafy vegetation cover on land (also called 'greenness' cover) for more than 20 years (Myneni and others 1998). Like the normalized difference vegetation index (NDVI), FPAR is a common measure of greenness cover (Knyazikhin and others 1998), ranging from zero (on barren land) to 100% (for dense cover). In theory, the higher the FPAR level observed over the course of a seasonal plant growing cycle, the denser the green leaf cover and (presumably, on average) the less disturbed the vegetation cover, and/or the longer the time period since the last major disturbance. It is plausible that any significant and sustained decline in vegetation FPAR observed from satellites represents a disturbance event, a hypothesis we evaluated here using independent records of such disturbance events

throughout North America. It is also possible that extreme climate events, such as droughts or cold waves, that occur during the same season of the year, but are separated by 9–12 months in two consecutive yearly cycles could result in a lower than average FPAR over the period of impact. Hence, it is possible to expand the definition of an ecological disturbance to include consecutive years of unfavorable growing season conditions for a given plant cover.

This study was conducted to evaluate patterns in a 19-year (1982–2000) record of satellite AVHRR observations of vegetation phenology over North America as a means to characterize major ecosystem disturbance events and regimes at a spatial resolution of 8-km, or pixel sizes of about 64 km². The same AVHRR greenness data set was applied by Hicke and others (2002) to compute net primary productivity (NPP) in North America using the Carnegie-Ames-Stanford approach (CASA) carbon cycle model. Although it was found that annual NPP averaged 6.2 Pg C (1 Pg = 10^{15} g) and that regional trends in the CASA model NPP record varied substantially across the continent, this study by Hicke and others (2002) dealt only with one flux in the continental carbon cycle (the terrestrial NPP sink) and did not address ecosystem disturbances as a potential source of carbon return to the atmospheric pool of CO_2. In a more comprehensive study by Potter and others (2003b) using the NASA-CASA ecosystem model, annual NPP in North America was reported to vary between 6 and 7.5 Pg C per year over the period 1982–1999, and the terrestrial sink for atmospheric CO_2 was fairly consistent at between +0.2 and +0.3 Pg C per year.

METHODS TO DETECT AND UNDERSTAND MAJOR DISTURBANCE REGIMES

The AVHRR multi-year time series of vegetation dynamics makes it possible to move beyond single disturbance events to conduct studies of "disturbance regimes". A disturbance regime is defined according to the spatial, temporal, and qualitative nature of disturbance events occurring within any given ecosystem type (Heinselman 1973). A natural disturbance regime (such as a forest fire cycle) can be described in terms of spatial extent (hectares) and distribution (patchiness), as well as the frequency and seasonality of its occurrence over time, and its severity or intensity (that is, the energy released per unit area and time). We describe below an approach to better understand major ecosystem disturbance regimes on a global level
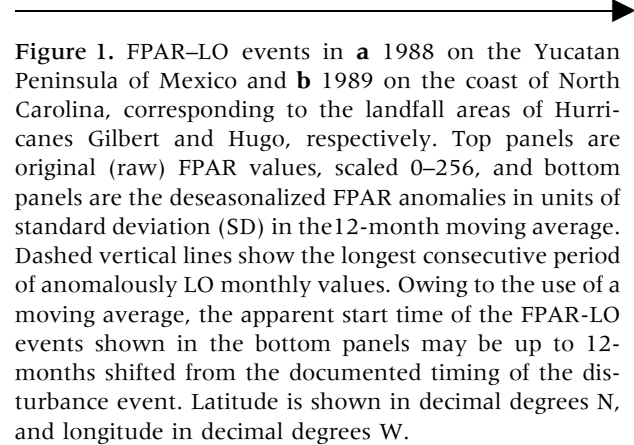
Figure 1. FPAR–LO events in **a** 1988 on the Yucatan Peninsula of Mexico and **b** 1989 on the coast of North Carolina, corresponding to the landfall areas of Hurricanes Gilbert and Hugo, respectively. Top panels are original (raw) FPAR values, scaled 0–256, and bottom panels are the deseasonalized FPAR anomalies in units of standard deviation (SD) in the 12-month moving average. Dashed vertical lines show the longest consecutive period of anomalously LO monthly values. Owing to the use of a moving average, the apparent start time of the FPAR-LO events shown in the bottom panels may be up to 12-months shifted from the documented timing of the disturbance event. Latitude is shown in decimal degrees N, and longitude in decimal degrees W.

using a 19-year record of monthly satellite-observed FPAR.

Monthly FPAR values for the land surface were derived from the AVHRR data sets covering the period 1982–2000. This FPAR data set was generated using canopy radiative transfer algorithms (Knyazikhin and others 1998), which are designed to generate improved vegetation products for input to terrestrial carbon flux calculations. These radiative transfer algorithms, developed for the moderate resolution imaging spectroradiometer (MODIS) aboard the NASA Terra satellite platform, account for attenuation of direct and diffuse incident radiation by solving a three-dimensional formulation of the radiative transfer process in vegetation canopies. Monthly composite data from channels 1 (visible) and 2 (near-infrared) of the AVHRR have been processed according to the MODIS radiative transfer algorithms and aggregated over the global land surface to 8-km spatial resolution. This aggregation level generates single grid cell (pixel) areas of approximately 6.4×10^3 ha (1 ha = 10^4 m²).

The observed FPAR time series at each pixel was first detrended (see example in Figure 1a) using a linear adjustment, which is necessary to minimize the possibility that, in cases where there is a gradual but marked increase in monthly FPAR over the 18-years time series, any potential disturbance events occurring relatively near the end of the series are not overlooked. To remove the dominant seasonal oscillations in vegetation phenology observed throughout the globe, our detrended FPAR time series was subsequently 'deseasonalized' by computing the 12-month running average time series for every pixel location.

An algorithm was next developed to identify any significant and sustained declines in FPAR during the time series.

a   FPAR at latitude = 20.55, longitude = -86.75

12-month moving average (count=15 months)

b   FPAR at latitude = 32.92, longitude = -79.90

12-month moving average (count=18 months)
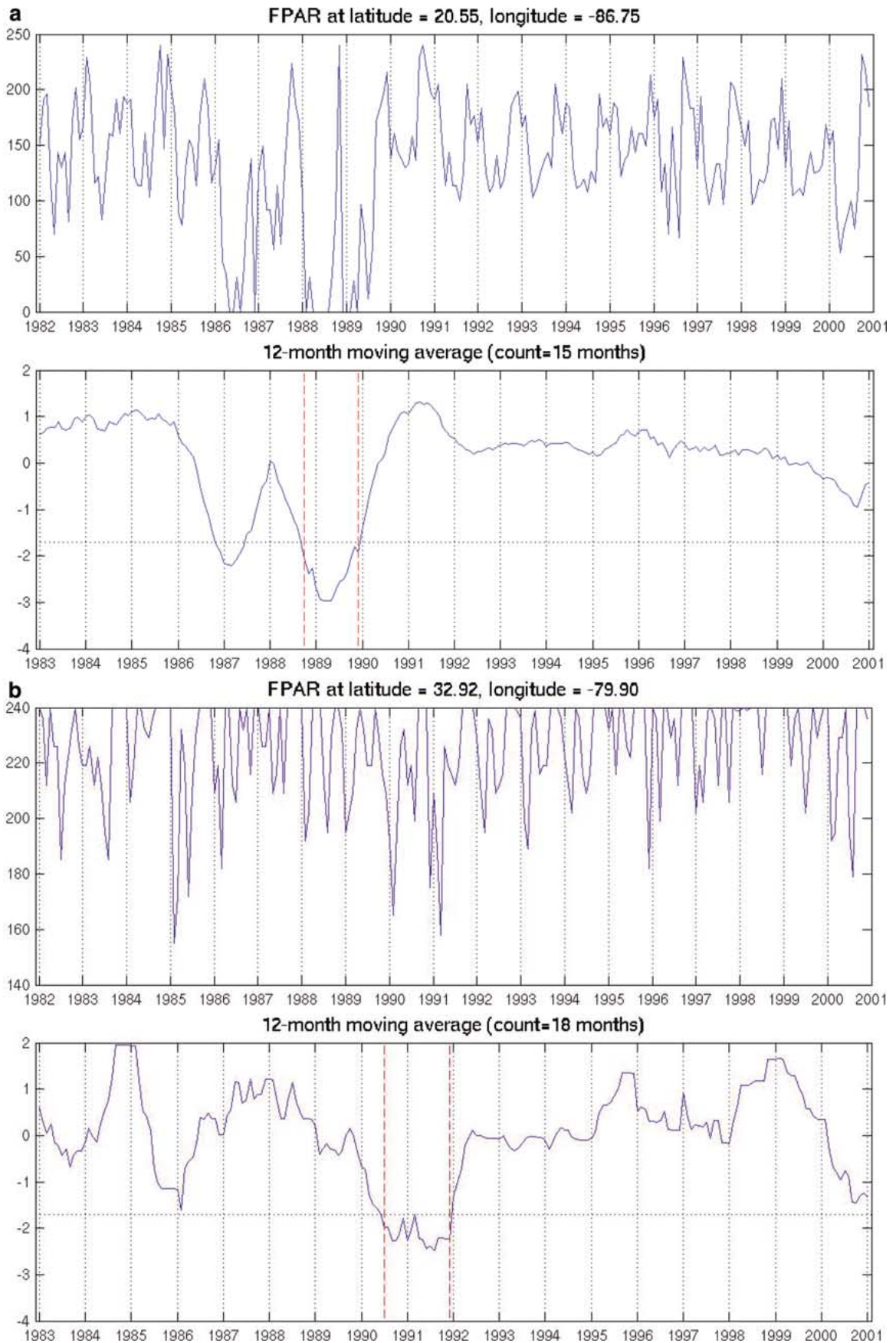
$$LSED = IF\ (FPARsd > 1.7)\ for \geq$$
$$12\ MOc\ THEN\ 1\ ELSE\ 0 \qquad (1)$$

where FPARsd is the number of standard deviations below the 18-years average monthly FPAR, and MO_c is the number of consecutive months in the 18-yr time series. Using a global 0.5° latitude/longitude FPAR data set, the algorithm was tested with a newly compiled data set of majored documented wildfires and cropland production failures worldwide from 1982 to 1998 and was found to have a sensitivity of successful event detection at disturbance area thresholds of at least 0.1 Mha in the polar zones to 0.3 Mha at the equator (Potter and others 2003a).

We hypothesized that significant declines in average annual FPAR levels can be defined to be greater than 1.7 standard deviations (SD) below (LO) the 18-years average FPAR computed for any specific pixel location. A "sustained" disturbance event would be defined as any decline in average annual FPAR levels (at an assigned significance level) that lasts for a temporal threshold value of at least 12 consecutive monthly observations at any specific pixel location. The logic used here is that an actual disturbance involves a sustained decline in FPAR because the structure of the vegetation cover has been severely altered or destroyed during the disturbance event, to a magnitude that lowers FPAR significantly for at least one seasonal growing cycle, after which time regrowth and recovery of the former vegetation structure may permit FPAR to increase again.

It is assumed that fairly common effects of atmospheric interference with the AVHRR channel signals, such as heavy cloud cover or smoke-derived aerosols, would not persist (for example, as a false disturbance event) in the multi-year time series and thereby generate a FPAR-LO pattern longer than about 6 months. By design, our disturbance algorithm should be insensitive to heavy cloud cover or smoke effects that occur practically every year during the same season, or only episodically for 1 or 2 months at a time. If an interference effect occurs every year at about the same time, it will be eliminated automatically as part of the deseasonalization algorithm. One possible exception to this principle could be persistent atmospheric interference effects generated by major volcanic eruptions, such as the Pinatubo event of late 1991.

Although it may be the case that FPAR can vary from year to year during dormant (non-growing) seasons, it is also possible for actual disturbances to occur during the dormant season, such as ice damage or an extremely low snow season. Dormant season events may also affect the quality of the following leaf-out and green-up periods in the growing season. Therefore, we cannot justify excluding the dormant season from our time series analysis. Furthermore, periodic errors in leafless canopy (versus full canopy) estimates of FPAR are not likely to have a major impact on the long-term (19-year) 12-month running mean FPAR, against which we have detected any and all of the FPAR-LO events.

In the use of a one-sided (LO) statistical t-test, rejection of the null hypothesis means that there is no difference between the 19-years average for the monthly FPAR level and the consistent FPAR-LO level identified in a string of 12 or more consecutive time steps. An absolute value SD of 1.7 or more represents the 95% LO confidence level, SD of 2.0 or more represents the 97% LO confidence level, and SD of 2.6 or more represents the 99% LO confidence level (Stockburger 1998). Because we have first detrended the FPAR time series by linear regression, the resulting data series should more closely approximate a normal distribution. The resulting data series have 18 degrees of freedom for tests of significance (19 years – 1 for a one-tailed test).

CONTINENTAL RESULTS FROM THE FPAR TIME SERIES

We applied the methods described above to the 1982–2000 FPAR time series from AVHRR observations at 8-km resolution to identify potential LSED events in terrestrial ecosystems of North America, which we assume to include the nations of the region commonly referred to as Central America. At a level of SD of 1.7 or more (95% confidence) for definition of disturbance intensity, we can detect 11,972 pixel locations at the threshold of 12 consecutive monthly time steps for FPAR-LO events (Figure 2a). For all vegetated land areas of North America, the fraction of total land area that had at least one FRAR-LO event was 3.9%. Summed over 19 years, these pixels together cover a total area of just over 766,000 km^2, which is slightly larger than the state of Texas. We hypothesize from these results that each of these pixels identified in Figure 2a has been affected to some degree by at least one LSED over the past two decades.

Geographic Distribution Patterns

The distribution with latitude of all pixel areas detected at a SD of 1.7 or more level lasting more than

Figure 2. a Distribution throughout North America of 8-km pixels as the first month and year for FPAR-LO lasting more than 12 consecutive months within the time series 1982–2000. **b** Continental sub-regions are listed as column headings in Table 1. Codes for sub-regions are GLK, Great Lakes; PNW, Pacific Northwest; WUS, Western United States; SEG, Southeast and Gulf of Mexico; NES, Northeast; CCA, Central Canada; ALK, Alaska.

12 consecutive months of FPAR-LO shows potential LSED events detected from northern arctic extremes of 78°N, throughout the middle latitudes, and down to the continental southern extreme at 6°N. The distribution among major global vegetation classes [delineated for this study according the 2001 MODIS land cover product from Friedl and others (2002)] of pixel areas from FPAR-LO events (Figure 2a) at SD of 1.7 or more indicates that 52% of continental LSED areas were located in forested ecosystems (mainly in evergreen and mixed coniferous-deciduous forests), whereas 28% were located in savanna and shrubland ecosystems (Table 1). Only about 20% of continental LSED areas were located in grassland and cropland ecosystems combined.

Table 1.   Percentages of FPAR-LO Events (8-km pixel resolution) in Vegetation Cover Classes for North America as a Whole and for Selected Sub-regions over the Period 1982–2000.

Vegetation class	Fraction of class	Percentage FPAR-LO pixels							
		NAM	GLK	PNW	WUS	SEG	NES	CCA	ALK
Mixed wetland	4.8	11	12	5	2	26	19	10	31
Evergreen needleleaf forest	4.8	24	14	54	2	3	13	50	5
Evergreen broadleaf forest	2.8	5	0	0	0	30	0	0	0
Deciduous needleleaf forest	>0.1	0	0	0	0	0	0	0	0
Deciduous broadleaf forest	1.4	2	7	0	0	0	18	0	0
Mixed forest	4.0	11	28	12	0	1	26	21	25
Closed shrubland	3.1	1	0	0	0	0	0	0	14
Open shrubland	3.1	23	0	17	70	2	0	10	20
Woody grassland/savanna	2.4	4	0	5	6	5	1	0	3
Savannas	1.5	1	0	0	2	3	1	0	0
Grasslands	2.9	8	0	6	16	5	0	3	1
Croplands	2.8	11	39	2	2	24	22	3	0

"Fraction of Class" percentages were computed as the number of FPAR-LO events compared to the total number of 8-km pixels in North America for vegetation classes delineated according the 2001 MODIS land cover product from Friedl and others (2002). Other percentages are computed as number of FPAR-LO events within each region, broken down by vegetation cover classes. Column percentages for sub-regions total to 100.
Barren (desert) and urban lands make up less than 1% of the FPAR-LO pixel total in all regions. Column heading codes: NAM, North America; and sub-regions GLK, Great Lakes; PNW, Pacific Northwest; WUS, Western United States; SEG, Southeast and Gulf of Mexico; NES, Northeast; CCA, Central Canada; ALK, Alaska. See Figure 2b for sub-region area boundaries.

As discussed briefly by Potter and others (2003a), our LSED detection method based on FPAR-LO events is best suited to ecosystems where there is a predominance of perennial woody vegetation cover in the region. Forests and shrublands recover relatively slowly from a sudden loss of green leaf cover, at least in contrast to grasslands and cultivated ecosystems, where a notable fraction of the green leaf biomass (and hence the FPAR) that is lost during a disturbance can be recovered fairly rapidly through herbaceous sprouting and plant regrowth during the same year as the disturbance event. Nonetheless, the results shown in Table 1 indicate that our LSED detection frequency is just as high within grassland and cropland classes as it is within certain forested vegetation classes. Hence, there is no overriding bias to forested vegetation in the FPAR-LO detection method.

On a sub-continental basis, all ecoregions within North America (Figure 2b) showed forests and tundra shrublands as the primary vegetation types where the FPAR-LO algorithm detected potential LSED events, lead by the Pacific Northwest, Alaska, and Central Canada with fewer than 10% FPAR-LO events detected in areas dominated by grasslands and croplands (Table 1). The Great Lakes region showed the highest proportion (39%) of FPAR-LO pixels detected in cropland areas, followed by the eastern U. S. ecoregions with over 20% coverage of FPAR-LO pixels in cropland areas.

The western U. S. ecoregion showed the highest proportion (16%) of FPAR-LO pixels detected in grassland areas.

Temporal Variations

When viewed in terms of the consecutive monthly time steps for FPAR-LO more than 12 months, the distribution of total pixel area at SD of 1.7 or more shows that 95% of the potential LSED coverage had a duration of between 12 and 20 consecutive months for FPAR-LO events (Figure 3). Beginning from the maximum concentration of pixel areas at 13 consecutive months (34% of all FPAR-LO pixels), the decline in area coverage with an increase in the number of consecutive monthly time steps was nearly exponential ($R^2 = 0.97$), out to the maximum value of 28 consecutive months of FPAR-LO. We could detect no significant trends in the relationship between latitude zone and number of consecutive monthly time steps for FPAR-LO events at SD of 1.7 or more. However, all of the longest FPAR-LO events of between 26 and 28 consecutive months for FPAR-LO were detected at latitude zones south of 52°N.

The distribution according to the start month for pixel areas detected at the SD of 1.7 or more level of FPAR-LO lasting more than 12 consecutive months shows that the periods of highest detection frequency were 1987–1989, 1995–1997, and 1999
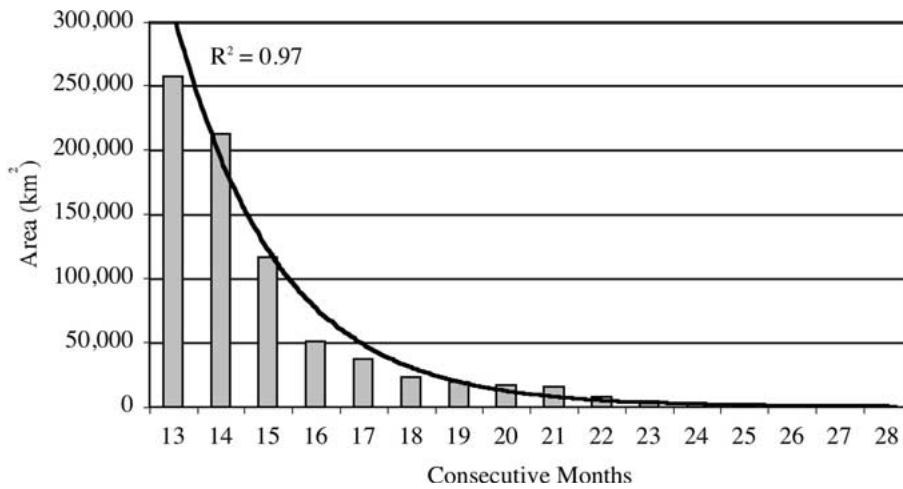
Figure 3. Distribution according to consecutive monthly time steps of land area detected with at least one FPAR-LO event in the time series 1982–2000.
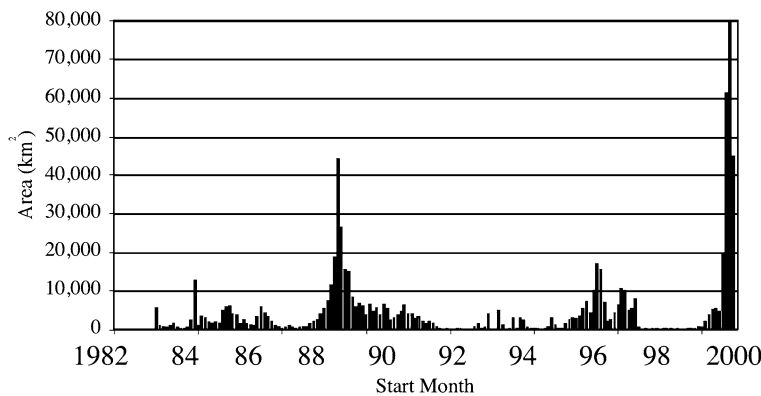
Figure 4. Distribution according to start month of land area detected with at least one FPAR-LO event in the time series 1982–2000.

(Figure 4). It is plausible that these time periods of high detection frequency for FPAR-LO events can be verified as coincident with major climate events during the time series. This kind of verification approach follows in a region-by-region examination of the patterns of potential LSED areas shown in Figures 2–4.

Reconstruction of Regional Ecosystem Disturbance Types

Verification of actual changes in ecosystems due to LSED events must be based on demonstrated relationships between the results shown in Figures 2, 3 and 4 and independently confirmed historical events, together with any major climate anomalies in the regions where potential LSED events are detected. In the topic sections that follow, we summarize regional disturbance types chronologically, with focus on well-documented tropical storms, wildfires, droughts, heat waves, cold waves, and blizzards during the 1980s and 1990s.

Tropical Storms of the 1980s

A series of major tropical storms in Category 3 or 4 (sustained winds in excess of 178 km per hr) made landfall across the southeastern coast of the United States and along the Gulf Coasts of the United States and Mexico during the 1980s (Table 2; Landsea 1993). By locating 8-km pixels in the vicinity of documented landfall points of storms (Powell and Aberson 2001), five of the strongest hurricanes making North American landfall in the 1980s were readily detected as FPAR-LO events in the 19-years AVHRR time series. These five hurricanes (in order of occurrence) were called Alicia, Elena, Gloria, Gilbert, and Hugo.

The impacts of Hurricane Gilbert in 1988 on the Yucatan Peninsula of Mexico and Hurricane Hugo in 1989 on the North Carolina coast (Figure 1) are representative of disturbance to forest ecosystems detected as FPAR-LO events throughout southeastern North America and Caribbean Islands during this period of severe tropical storm damage. The hurricane season in North America extends from

Table 2. Hurricanes (Category 3 and higher) of the 1980s Detected as FPAR-LO Events (after Powell and Aberson 2001)

Year	Hurricane	Category	Landfall location	Landfall Lat/Lon
1983	Alicia	3	SE Texas, USA	28.9°N 95.0°W
1985	Elena	3	Mississippi, USA	30.2°N 88.8°W
1985	Gloria	3	East Coast, USA	35.5°N 75.5°W
1988	Gilbert	3	East Coast, Mexico	20.4°N 86.5°W, 23.9°N 97.0°W
1989	Hugo	4	North Carolina, USA	33.5°N 80.3°W

June to November, with storms most common in September, when ocean temperatures are warmest. The FPAR time series in Figure 1 show this expected timing of FPAR-LO events detected in late summer or early autumn of 1988 and 1989.

Unlike the examples shown in Table 2, Hurricane Andrew, a Category 4 storm that struck southern Florida in 1992, could not be detected as a FPAR-LO event in the 19-years AVHRR time series. The probable explanation is that the landfall areas in southern Florida for Hurricane Andrew were not dominated by forest vegetation cover, but instead by grassland and wetland areas. Hence, the disturbance detection method with thresholds of SD of 1.7 or more FPAR-LO lasting more than 12 consecutive months will not reveal areas of predominantly annual herbeaceous cover that would only be disrupted for several weeks or a month due to a severe wind event.

Pacific Northwest Logging of the 1980s

The extent to which mature forests (>80 years old) have been disturbed in the Pacific Northwest (PNW) has been estimated at over 75% by the 1990s (NRC 2000), the majority of which is attributable to logging. The PNW states of Oregon (OR) and Washington (WA) are notable as having had relatively large forest logging and wildfire impacts during the 1980s. Additionally, repeated stand-replacing disturbances have been rare (0.03% of the forest area in OR) over the time frame of the past 30 years (Cohen and others 2002). These unique attributes of the PNW region facilitate comparisons of the FPAR-LO event patterns shown in Figure 2a with many large-scale forest disturbance events throughout OR and WA.

Cohen and others (2002) have developed a new set of Landsat-based maps for historical forest disturbance in OR and WA. These maps of stand-replacing forest disturbances in the Northwest Forest Plan area between 1972 and 2002 were generated using a change detection method that is approximately 90% accurate (Cohen and others

1998). Versions of these 30-m resolution maps were created following methods from Cohen and others (2002) and aggregated to 8-km spatial grids for OR and WA using extended geographic areas and time periods. Comparisons between our 8-km FPAR-LO pixels and the PNW Landsat-derived disturbance locations showed that the maximum disturbance area coverage in any 8-km grid cell for OR and WA was about 33%. Compared to 1984–1988 and 1988–1992 Landsat-derived maps for WA, we find that the FPAR-LO disturbance detection algorithm can reliably differentiate FPAR signatures in relatively disturbed (FPAR-LO at SD ≥ 2.0) versus non-disturbed forest areas for the region (Figure 5).

More specifically, Landsat products generated from the method of Cohen and others (2002) show disturbed forest cover in 95% of the 8-km pixels where our AVHRR algorithm detects an FPAR-LO event during the matching time period, provided that there is greater than 50% forest cover overall in the 8-km pixel area. Wherever the MODIS 1-km land cover map indicates that there is less than 50% forest cover in a 8-km resolution pixel, our result is less than a 20% match (8-km pixel-by-pixel for disturbed area cover) between the two disturbance mapping methods. Based on these results, we surmise that more than 50% forest cover is a reasonable lower cutoff for the differentiation of forest disturbance versus non-disturbance FPAR signatures in the AVHRR time series.

Droughts and Heat Waves

Dry hot weather events were common throughout the 1982–1998 time period in the south-central

Figure 5. FPAR monthly time series for single 8 km pixels in NW Washington state with **a** 4.3% disturbed forest area detected during the period 1984–1988, and **b** 0% disturbed forest area detected during the period 1984–1988 [determined from Landsat imagery according to the methods of Cohen and others (2002)]. Both pixels are in areas with more than 50% forest cover.

a   FPAR at latitude = 48.13, longitude = -123.91

12-month moving average (count=13 months)

b   FPAR at latitude = 47.97, longitude = -123.77

12-month moving average
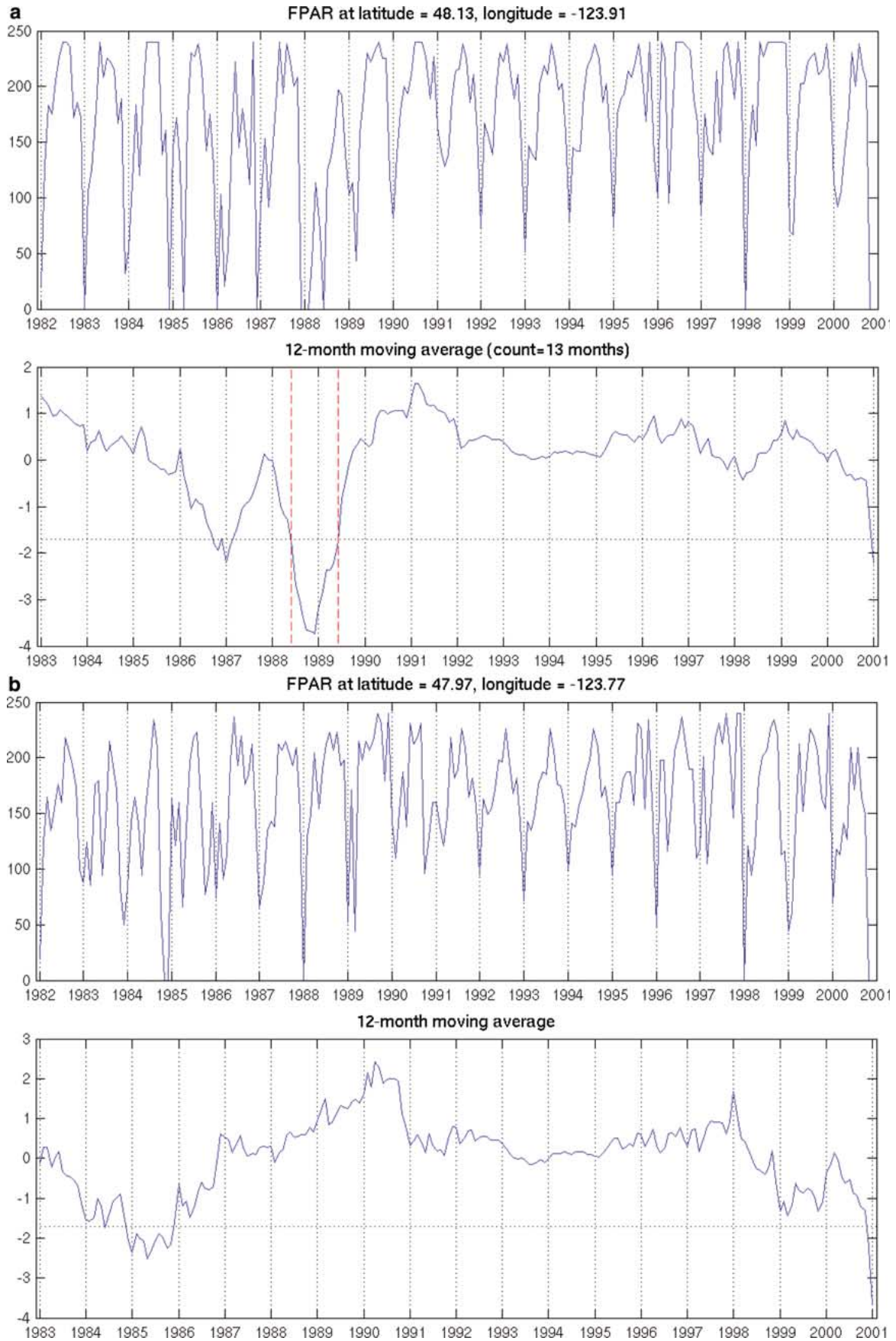
United States. The first regional summer drought and heat wave to occur in the 1980s affected large parts of the southeastern United States in 1986. Extreme July temperatures in Georgia, North Carolina, and South Carolina were the warmest recorded in the 20th century (Bergman and others, 1986; Karl and Young 1987). The unusually dry hot weather resulted in severe losses to agriculture.

In 1988, a severe summer drought affected the central and eastern United States. Dry weather began in April and persisted through June. Record high temperatures occurred throughout the summer in the midwest and northeastern regions, with many locations setting all-time records for June. Record numbers of forest fires broke out across the western United States, including the Yellowstone National Park fire (Renkin and Despain 1992). Again in 1989, severe summer drought over much of the northern plains resulted in significant losses to agriculture. Drought severely impacted the northwestern and southwestern parts of Colorado. At this same time, California was experiencing the third year of an historic 7-year drought (1986–1993).

During the June–July period of 1993, much of the southeastern United States received less than 50% of normal rainfall along with temperatures several degrees above normal. The southeast as a whole recorded the second driest July on record since 1895 (the driest was 1983). The states of Alabama, Georgia, North Carolina, South Carolina, Tennessee, and Virginia had their hottest July on record since 1895.

In 1998, drought and extreme heat affected a large area of the south-central United States from Texas and Oklahoma eastward to the Carolinas, Georgia, and Florida. Dry weather began in mid-March 1998. Many locations set daily maximum temperature records during the summer of 1998. Locations along the east coast of Florida set a number of high minimum records probably as a result of the insulating affect of the aerosols generated by wildfires and the abnormally warm waters in the Gulf of Mexico and Atlantic Ocean.

Impacts of each of these severe drought years can be detected in the start times and general locations of FPAR-LO events throughout the southeastern, central, and northern plains regions of the United States (Figure 2a). A time series example from North Carolina (Figure 6) illustrates the impact of repeated summer droughts and heat waves on the regional greenness profile. The start of the largest FPAR-LO event was detected early in 1986 and lasted for slightly longer than 12 months, followed by a gradual recovery during the next 2 years. The

drought of 1983 seems to have had an impact early in the FPAR time series, and the return of dry hot summer conditions could be detected a second time as the downturn of FPAR in 1993 through 1994, and a third time in 1998.

In some cases, slight increases in detection sensitivity revealed further evidence of drought-induced crop failures. For instance, we found that by reducing our SD of 1.7 or more threshold to SD of 1.5 or more, sensitivity of the disturbance detection algorithm was increased notably in croplands of the Midwestern states. The detection with a threshold of SD of 1.5 or more identified many more FPAR-LO pixels in Nebraska and South Dakota where the 1988 droughts appear to be the cause of extensive reduction in plant greenness.

Large-Scale Forest Fires

A critical set of historical disturbance events available for verification of FPAR-LO events as LSEDs are well-documented wildfires that burned areas reported to cover tens of thousands of hectares in a single year or growing season. A list of such events was compiled (Table 3) using publications and reports from the North American fire literature. The list in Table 3 is not intended to represent an exhaustive set of North American fire events over the 19-years period of the FPAR record, but instead is a list of the largest fire events that could be confirmed for their timing of initiation (to within about 3 months) and geographic location (to within approximately 1° latitude and longitude). Selected wildfire areas have been confirmed for timing and location using Landsat and other relatively high resolution satellite images (Arino and Plummer 1999).

We find that within each geographic area of the confirmed wildfire events listed in Table 3, an FPAR-LO event was detected during the reported time period of actual wildfire activity. As an example, the FPAR time series for the Yellowstone National Park fire (Figure 7) shows a significant FPAR-LO event (SD ≥ 2.0) beginning during the summer of 1988. This pixel location coincides with the North Fork Fire that spread on the edge of the Park toward West Yellowstone, Montana. The recovery back to long-term average FPAR required nearly 2 years.

Cold Wave and Blizzards of 1995–1997

According to the U. S. National Weather Service, the winter of 1995–1996 featured abnormally cold and snowy conditions in Canada and United States. For the winter season as whole, temperatures
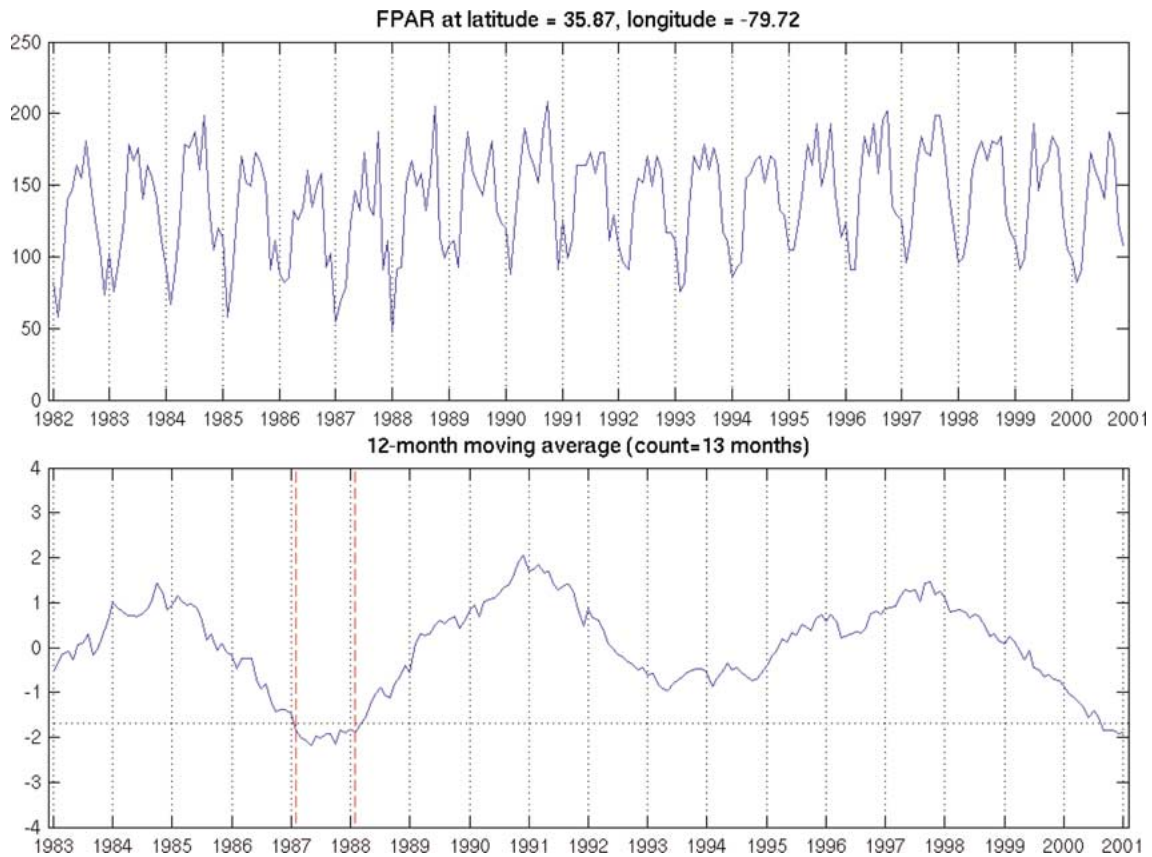
Figure 6. FPAR–LO event in North Carolina 1986, showing drought and heat wave impacts on southeastern U.S. greenness profiles.

Table 3. List of Major Forest Wildfires on Record for North America in the 1980s and 1990s

Year	Location	Area Burned (ha)	Lat/Lon	Notes
1987	Stanislaus, California USA	59,000	38°N 120°W	Stanislaus National Forest
1987	Siskiyou,Oregon USA	51,000	42°N 124°W	Silver fire, Siskiyou National Forest
1988	Yellowstone, Wyoming USA*	> 500,000	44.6°N 110.7°W	
1989	Manitoba, Canada	>400,000	51°N 97°W	Lake Manitoba, spread northward for 800 km
1989 and 1991	Quebec, Canada	> 200,000	52°N 75°W	
1997	Alaska USA	>200,000	63–64°N 159°W	Inowak fire (100 miles SW of McGrath), Simels and Magitchlie Creek fires Galena District
1998	Mexico*	> 500,000	17–22°N 94°–98°W	Chiapas, Oaxaca

Sources: Weatherspoon and Skinner (1995); Jeffrey (1989); Kasischke and others (1999); Galindo and others. (2003); Canadian Interagency Fire Center (2001) Reports, Winnipeg, Manitoba
*Fire location has been confirmed using Landsat and ATSR (Along Track Scanning Radiometer) satellite images (Arino and Plummer 1999)

averaged 3–5°C below normal across central Canada, and 1–2°C below normal across the northern tier of the United States. Arctic airmass movement began in late January 1996 across the northern plains and northern Rockies. The most notable cold wave occurred during early February 1996, when
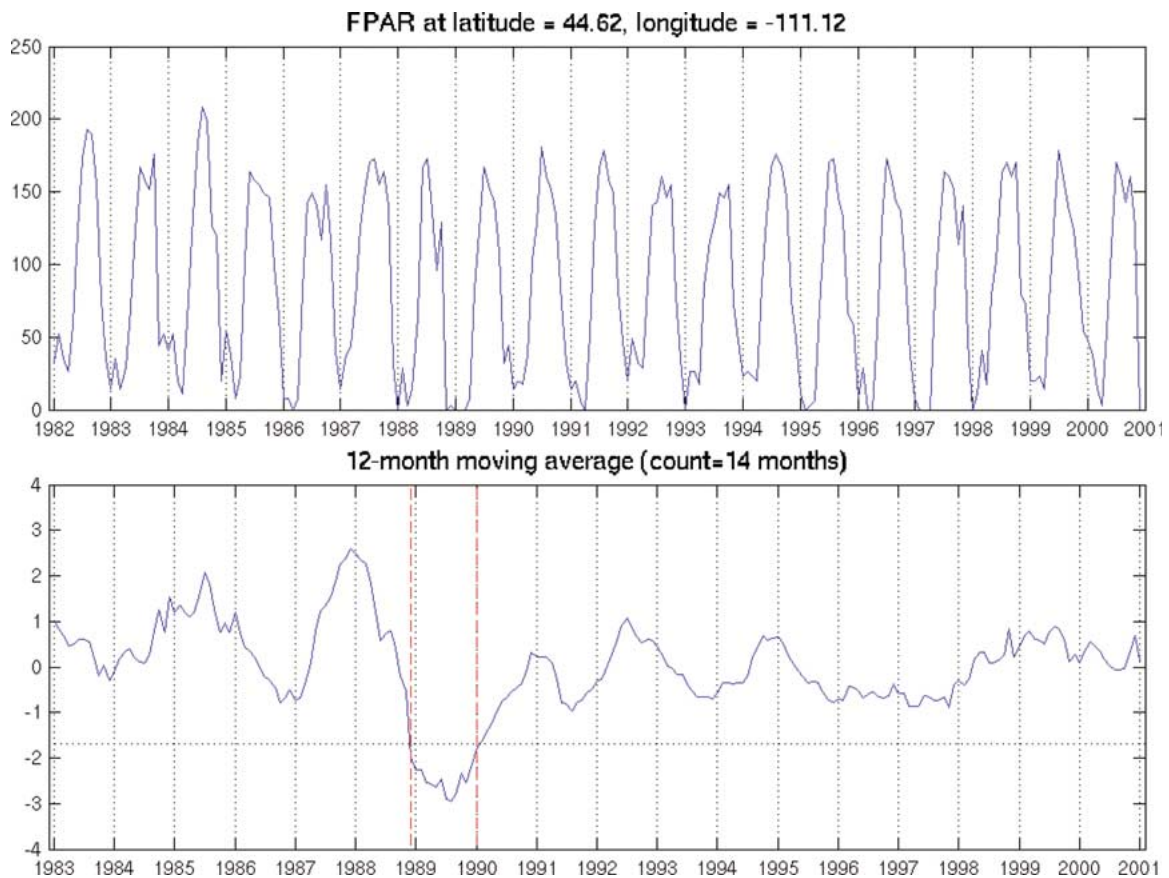
Figure 7. FPAR–LO event in the summer of 1988, centered several kilometres south of West Yellowstone, Montana at the North Fork Fire locations spreading from Yellowstone National Park.

temperatures averaged 11–17°C below normal from the southern Canadian prairies southeastward to the western Great Lakes. The Midwestern Climate Center reported that in four states (Illinois, Iowa, Minnesota, Wisconsin) this was one of coldest weather events of the 20th Century.

In the first week of January, 1996, much of the eastern seaboard received from 1 to 3 feet of snow during the "Blizzard of '96". Snowfall totals by the end of February 1996 averaged more than 150% of normal across the upper midwestern United States. The Aviation Weather Center of Kansas City, MO and Intellicast reported extensive tree damage in the north-central United States due to the heavy, wet nature of the snow fall. The winter of 1996–1997 brought a second consecutive season of unusually heavy snowfall across the upper Midwestern states, with 2–3 times the mean annual amounts.

Impacts of these two consecutive cold waves in 1996 and 1997 could be detected in the start times and general locations of FPAR-LO events throughout lower Wisconsin, Michigan, and southwestern Ontario, and over much of south-central Canada (Figure 2a). A time series example from Wisconsin (Figure 8) demonstrates the impact of extended winter conditions into the spring seasons of 1996 and 1997 on the regional greenness profile. The seasonal pattern of monthly greenness values for these pixels suggests a significant delay in the spring 'green-up' in both 1996 and 1997, compared to all the other spring seasons in the 19-years FPAR time series. Instead of a typical rapid greening from March to May, both 1996 and 1997 showed a 1–2 month delay in spring greening and a shorter growing season overall. The 1996 spring-summer growing season was the shortest of all, whereas the end of the 1997 spring-summer growing season tends back toward an average year duration.

As shown in Table 1, about 60% of the 8-km pixels in the Great Lakes region that show the extended decline in mean greenness over 1996–1997 were classified as predominantly coniferous and mixed forest cover (including wetlands). The remaining 40% of the pixels were classified as
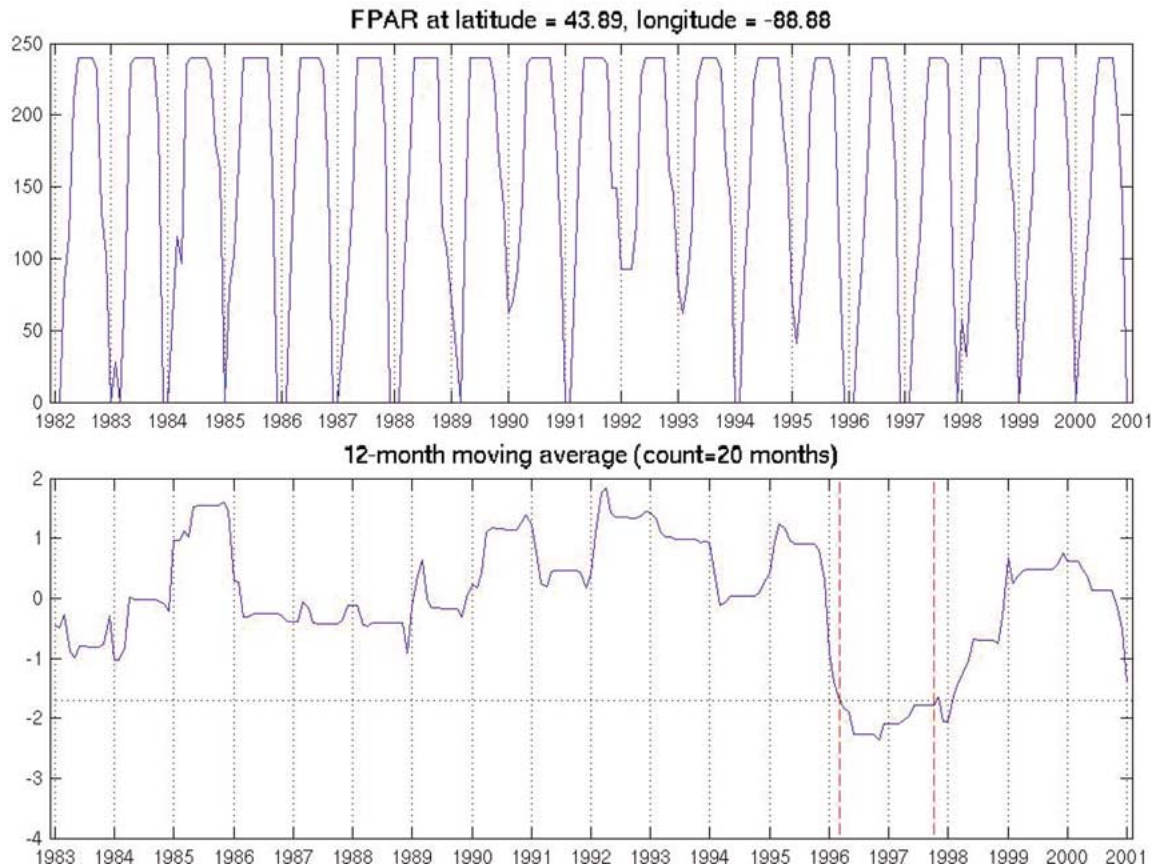
Figure 8. FPAR–LO event in Wisconsin 1996–1997, showing 2 consecutive years of winter-spring cold wave impacts on midwestern U.S. greenness profiles.

predominantly cropland cover, although many stands of trees will be mixed with crop cover at the 8-km pixel resolution. Because the 1996–1997 Great Lakes FPAR-LO anomaly was detected in many different vegetation types, this suggests regional climate phenomena at work, rather than a species-specific production decline in just one type of plant cover.

To corroborate these anomalies in FPAR-LO patterns throughout the Great Lakes region, we examined 21-year (1980–2000) monthly and daily climate records at 0.5° latitude × 0.5° longitude resolution (New and others 2000; Kistler and others 2001). Annual growing degree day (GDD; base 8°C) anomalies for 1996 and 1997 (relative to the 1980–2000 annual averages) show that plant growth was likely slowed. Lower than average GDD accumulations were observed during 1996 and 1997 over most of Michigan, southwestern Ontario, and in lower Wisconsin (Figure 9). Numerical simulations with an agroecosystem model (Kucharik 2003) suggested that a key limitation to crop development during these two years

could have been a delayed spring planting date of 20–25 days compared to optimal planting dates in these same regions (JA. Foley and others, submitted).

Although we can characterize the observed FPAR-LO patterns throughout the Great Lakes region during 1996–1997 as a LSED, this type of anomaly in the satellite greenness record may not involve a conventional destruction of forest wood biomass that is typical of a wildfire or a hurricane. Rather, 2 consecutive years of lower than average growing season length and decreased GDD accumulations due to prolonged winter seasons would represent a similar disruption in annual productivity that is traceable to the slow phenologic responses illustrated in Figure 8.

Western Canadian Drought and Heat Wave of 1999–2000

An extensive coverage of FPAR-LO events is notable (Figure 2a) starting in late 1998 and early 1999 over the Pacific coastal regions of Canada and
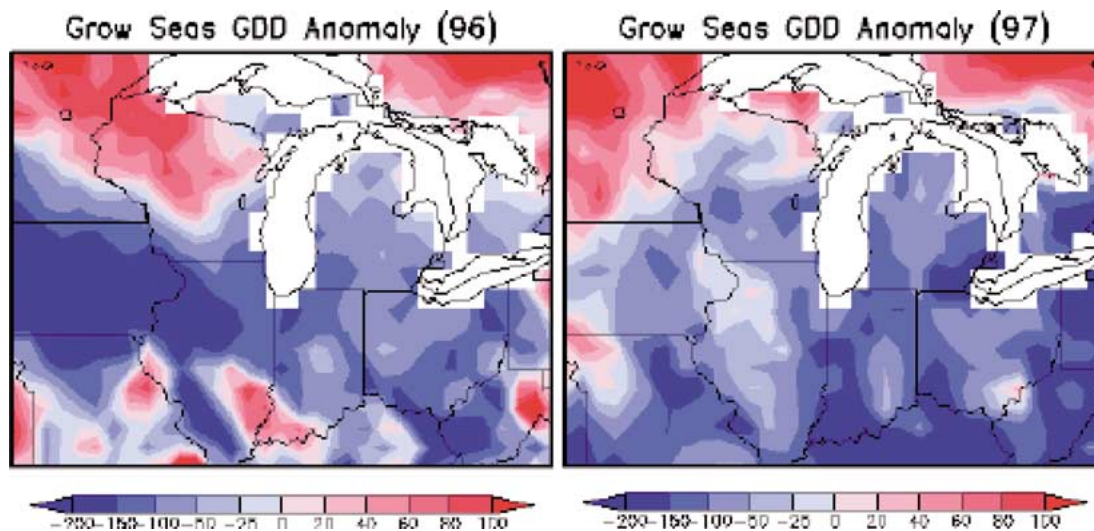
Figure 9. Anomalies in growing season (defined as the time period from the last spring freeze to the first fall freeze, inclusive, using 0°C as a temperature threshold) growing degree days (GDD, base 8°C) for 1996 (*left*) and 1997 (*right*).

the boreal mountain zones of British Columbia and the Yukon. The most probable explanation for a LSED event in the region is extreme drought and heat waves. The Meteorological Service of Canada reported that 1998 was one of the driest and warmest summers in the past 55 years (−41% lower rainfall and +1.3°C higher temperature, compared to averages over 1948–2003) for the region of the northern British Columbia Mountains and the Yukon (Environment Canada 1999). A second consecutive heat wave followed in the summer of 1999, particularly along the Pacific Coast region of Canada, with temperatures 1.2°C above the same long-term annual mean.

The 1998–1999 LSED event in British Columbia may also be linked to recent outbreaks of bark beetles (Logan and Powell 2001) in forests dominated by pine, spruce, or fir species. These wood-boring insects favor mild (warm) winters and then typically spread in search of new tree food sources in July and August, when trees are most vulnerable to infestation due to water deficiency. Damage done by the bark beetles can eventually kill trees, turning green leaf canopies to brown over large areas, and subsequently increasing the risk of wildfire.

CONCLUSIONS

A main objective of this study was to better understand historical patterns of ecosystem disturbance events throughout North America and to characterize major disturbance regimes in terms of spatial extent, geographic distribution, and fre-quency over time. To this end, we are able to draw several conclusions on the basis of results from the analysis of the 19-years FPAR time series from AVHRR observations.

First, our method to detect LSED using satellite greenness images is most effective in places where there is a predominance of perennial forest or shrub vegetation cover. In grasslands and cultivated ecosystems, green leaf biomass is produced annually and any leaf cover that is altered during a disturbance could be recovered in large part through regrowth during the same season or year as the disturbance event. Consequently, our method of defining FPAR-LO events is designed to perform best in the detection of major disturbances in forest and shrubland ecosystems, where biomass storage in perennial woody tissues may be lost or damaged in fires, hurricanes, or logging operations. This is especially applicable where green leaf cover in the canopy cannot regenerate fully during the same year as the disturbance event. In the case of prolonged droughts, heat waves, or herbivorous insect outbreaks, our FPAR-LO methods can detect major disturbances in grasslands and cultivated ecosystems, as well as in forested areas.

Second, the widespread impacts of repeated winter cold waves and delayed springtime warming suggest that these events can contribute to regional disturbance regimes on a geographic scale similar to that of major summer droughts and heat waves. Although there may be a need for further validation of the causes for observed FPAR-LO patterns throughout the Great Lakes region during 1996–1997, the large spatial coverage of this potential

LSED event has not been reported previously in any public documents known to us.

Third, several notable limitations exist in the use of satellite image pixels as coarse as 8-km resolution. Small-scale logging and partial tree removal activities cannot be detected reliably at this resolution. The same can be said for wildfires smaller than 6,400 ha of area burned. Flooding along major rivers is likely to be localized in its disturbance impacts, and therefore not detected at this resolution. Ice storms and localized wind storms seem to fall into this same category of being below the 8-km detection level for effects on satellite FPAR.

In closing, we suggest that the historical AVHRR satellite greenness record holds numerous undiscovered patterns that may change scientific views of continental and global alterations in the land surface over the past 20 years. In North America alone, a picture is emerging of periodic droughts and heat waves, possibly coupled with herbivorous insect outbreaks, as among the most important causes of ecosystem disturbance in recent times. If temperatures continues to warm over interior forested areas of the continent, the results presented in this paper may be a useful baseline against which to compare future changes in large-scale disturbance regimes.

ACKNOWLEDGEMENTS

REFERENCES

Amiro BD, Todd JB, Wotton BM, Logan KA, Flannigan MD, Stocks BJ, Mason JA, Martell DL, Hirsch KG. 2001. Direct carbon emissions from Canadian forest fires, 1959–1999. Can J For Res 31:512–25.

Andreae MO. 1991. Biomass burning: its history, use, and distribution and its impact on environmental quality and global climate. In: Levine JS, Eds. Global Biomass Burning: Atmospheric, Climactic and Biospheric Implications. New York: MIT Press. p 3–21.

Arino O, Plummer S. 1999. Along track scanning radiometer world fire atlas: validation of the 1997–1998 active fire product. IGBP Report.

Barbosa, PM, Grégoire J-M, Stroppiana D, and Pereira JMC, 1999. An assessment of fire in Africa (1981–1991): Burnt biomass and atmospheric emissions. Global Biogeochemical Cycles, 13:933–950.

Bergman KH, Ropelewski CF, Halpert MS. 1986. The record southeast drought of 1986. Weatherwise 39:262–6.

Canadell JG, Mooney HA, Baldocchi DD, Berry JA, Ehleringer JR, Field CB, Gower ST, Hollinger DY, Hunt JE, Jackson RB, Running SW, Shaver GR, Steffen W, Trumbore SE, Valentini R, Bond BY. 2000. Carbon metabolism of the terrestrial biosphere: a multi-technique approach for improving understanding. Ecosystems 3:115–30.

Canadian Interagency Forest Fire Centre (CIFFC). 2001. Canada Report 2001, Winnipeg, Canada. p 6.

Cohen WB, Fiorella M, Gray J, Helmer E, Anderson K. 1998. An efficient and accurate method for mapping forest clearcuts in the Pacific Northwest using Landsat imagery. Photogram Eng Remote Sens 64:293–300.

Cohen W, Spies T, Alig R, Oetter D, Maiersperger T, Fiorella M. 2002. Characterizing 23 years (1972–1995) of stand replacement disturbance in western Oregon forests with Landsat imagery. Ecosystems 5:122–137.

DeFries R, Townshend J. 1994. NDVI-derived land cover classification at global scales. Internl J Remote Sens 15:3567–86.

Environment Canada. 1999. Climate Trends and Variations Bulletin for Canada, Atmospheric Environment Service Downsview, Ontario, p 2.

Fearnside PM. 1997. Greenhouse gases from deforestation in Brazilian Amazonia: net committed emissions. Clim Change 35:321–60.

Friedl MA, McIver DK, Hodges JCF, Zhang XY, Muchoney D, Strahler AH, Woodcock CE, Gopal S, Schneider A, Cooper A, Baccini A, Gao F, Schaaf C. 2002. Global land cover mapping from MODIS: algorithms and early results. Remote Sens Environ 83:287–302.

Galindo I, Lopez Perez P, Evangelista Salazar M. 2003. Real-time AVHRR forest fire detection in Mexico (1998–2000). Int J Remote Sens 24:9–22.

Heinselman ML. 1973. Fire in the virgin forests of the Boundary Waters Canoe Area, Minnesota. Quaternary Res 3:329–82.

Hicke JA, Asner GP, Randerson JT, Tucker CJ, Los SO, Birdsey R, Jenkins JC, Field CB, Holland EA. 2002. Satellite-derived increases in net primary productivity across North America, 1982–1998. Geophys Res Lett 29(10):1427, doi:10.1029/2001GL013578.

Houghton RA, Hackler JL, Lawrence KT. 1999. The U.S. carbon budget: contributions from land-use change. Science 285:574–9.

Houghton RA. 1999. The annual net flux of carbon to the atmosphere from changes in land use 1850–1990. Tellus 51B:298–313.

Houghton RA, Lawrence KT, Hackler JL, Brown S. 2001. The spatial distribution of forest biomass in the Brazilian Amazon. Glob Change Biol 7:731–46.

Houghton RA, Hackler JL. 1999. Emissions of carbon from forestry and land-use change in tropical Asia. Glob Change Biol. 5:481–92.

Hurst DF, Griffith DWT, Cook GD. 1994. Trace gas emissions from biomass burning in tropical Australian savannas. J Geophys Res 99:16441–56.

Jeffrey D. 1989. Yellowstone: the great fires of 1988. Natl Geogr 175:255–73.

Karl TR, Young PJ. 1987. The 1986 Southeast drought in historical perspective. Bull Am Meteorol Soc 68:773–8.

Kasischke ES, French NHF, Bourgeau-Chavez LL. 1999. Using satellite data to monitor fire-related processes in boreal forests.

In: Kasischke ES, Stocks BJ, Eds. Fire, Climate Change and Carbon Cycling in the Boreal Forest, Ecological Studies Series. Berlin, Heidelberg New York: Springer. p 406–22.

Kistler R, Kalnay E, Collins W, Saha S, White G, Woollen J, Chelliah M, Ebisuzaki W, Kanamitsu M, Kousky V, van den Dool H, Jenne R, Fiorino M. 2001. The NCEP-NCAR 50–year reanalysis. Bull Amer Meteorol Soc 82:247–68.

Knyazikhin Y, Martonchik JV, Myneni RB, Diner DJ, Running SW. 1998. Synergistic algorithm for estimating vegetation canopy leaf area index and fraction of absorbed photosynthetically active radiation from MODIS and MISR data. J Geophys Res 103:32257–76.

Kucharik CJ. 2003. Evaluation of a process-based agro-ecosystem model (Agro-IBIS) across the U.S. cornbelt: simulations of the inter-annual variability in maize yield. Earth Interact 7:1–33.

Kurz WA, Apps MJ. 1999. A 70–years retrospective analysis of carbon fluxes in the Canadian forest sector. Ecol Appl 9:526–47.

Landsea C. 1993. A climatology of intense (or major) Atlantic hurricanes. Mon Weather Rev 121:1703–13.

Logan JA, Powell JA. 2001. Ghost forests, global warming, and the mountain pine beetle. Am Entomol 47:160–73.

Murph PJ, Mudd JP, Stocks BJ, Kasischke ES, Barry D, Alexander ME, French NHF. 2000. Chapter 15: historical fire records in the North American boreal forest. In: Kasischke ES, Stocks BJ, Eds. Fire, Climate Change, and Carbon Cycling in the Boreal Forests. Berlin Heidelberg New York: Springer.

Myneni RB, Tucker CJ, Asrar G, Keeling CD. 1998. Interannual variations in satellite-sensed vegetation index data from 1981 to 1991. J Geophys Res 103:6145–60.

NRC (National Research Council)2000. Environmental Issues in Pacific Northwest Forest Management Washington (DC): National Academy Press.

Nepstad DC, Veríssimo A, Alencar A, Nobre C, Lima E, Lefebvre P, Schlesinger P, Potter C, Moutinho P, Mendoza E, Cochrane M, Brooks V. 1999. Large-scale impoverishment of Amazonian forests by logging and fire. Nature 398:505–8.

New M, Hulme M, Jones P. 2000. Representing twentieth century space-time climate variability. II. Development of 1901–1996 monthly grids of terrestrial surface climate. J Clim 13:2217–38.

Pickett STA, White PS. 1985. The Ecology of Natural Disturbance as Patch Dynamics. New York: Academic Press.

Potter CS. 1999. Terrestrial biomass and the effects of deforestation on the global carbon cycle. BioScience 49: 769–78.

Potter CS, Klooster SA, Brooks V. 1999. Interannual variability in terrestrial net primary production: exploration of trends and controls on regional to global scales. Ecosystems 2:36–48.

Potter CS, Brooks-Genovese V, Klooster SA, Bobo M, Torregrosa A. 2001. Biomass burning losses of carbon estimated from ecosystem modeling and satellite data analysis for the Brazilian Amazon region. Atmos Environ 35:1773–81.

Potter C, Tan P, Steinbach M, Klooster S, Kumar V, Myneni R, Genovese V. 2003a. Major disturbance events in terrestrial ecosystems detected using global satellite data sets. Glob Change Biol 9(7):1005–21.

Potter C, Klooster S, Myneni R, Genovese V, Tan P, Kumar V. 2003b. Continental scale comparisons of terrestrial carbon sinks estimated from satellite data and ecosystem modeling 1982–1998. Glob Planet Change 39:201–13.

Powell MD, Aberson SD. 2001. Accuracy of United States tropical cyclone landfall forecasts in the Atlantic basin 1976–2000. Bull Am Meteoro Soc 82:2749–67.

Renkin RA, Despain DG. 1992. Fuel moisture, forest type, and lightning-caused fires in Yellowstone National Park. Can Forestry Forest Res 22:37–45.

Schimel D, House J, Hibbard K, Bousquet P, Ciais P, Peylin P, Apps M, Baker D, Bondeau A, Brasswell R, Canadell J, Churkina G, Cramer W, Denning S, Field C, Friedlingstein P, Goodale C, Heimann M, Houghton RA, Melillo J, Moore III B, Murdiyarso D, Noble I, Pacala S, Prentice C, Raupach M, Rayner P, Scholes B, Steffen W, Wirth C. 2001. Recent patterns and mechanisms of carbon exchange by terrestrial ecosystems. Nature 414:169–72.

Scholes RJ, Kendall J, Justice CO. 1996. The quantity of biomass burned in southern Africa. J Geophy Res 101:23667–76.

Stockburger DW. 1998. Introductory Statistics: Concepts, Models, And Applications, WWW Version 1.0, http://www.psychstat.smsu.edu/sbk00.htm.

Tilman D. 1985. The resource-ratio hypothesis of plant succession. Am Nat 125:827–52.

Walker LR, Willig MR, Eds. 1999. Ecology of Disturbed Ground. Amsterdam: Elsevier.

Weatherspoon CP, Skinner CN. 1995. An assessment of factors associated with damage to tree crowns from 1987 wildfires in northern California. Forest Sci 41:430–51.